Clustering recognition model for intermediate energy heavy ion reactions

E. J. Garcia-Solis and A. C. Mignerey
Chemistry Department, University of Maryland, College Park, Maryland 20742
(Received 20 November 1995)

A clustering model which allows the recognition of mass fragments from dynamical simulations has been developed. Studying the evolution of a microscopic computation based on the nuclear Boltzman equation, a suitable time is chosen to define bound clusters. At this stopping time the cluster cores for each member of the distribution are defined as a function of the overall density. Then an iterative routine is applied to estimate the coalescence of the surrounding nucleons. Once the fragment formation has been established, a statistical decay code is used to generate the final fragment distributions. Applications are shown to the reactions ^{129}Xe + ^{nat}Cu at 50 MeV/nucleon and ^{139}La on ^{27}Al and ^{nat}Cu at 45 MeV/nucleon. A general improvement in cluster identification is found over approaches where a standard cluster separation algorithm has been used. [S0556-2813(96)03507-8]

PACS number(s): 24.10.Lx, 21.60.Gx, 25.70.Mn

I. INTRODUCTION

Microscopic simulations are fundamental to the study of the evolution of nuclear collisions at intermediate energies. These simulations permit the interpretation of experimental data and facilitate the extraction of information about the physical properties of hot and dense nuclear matter, such as multifragment emission or nuclear compressibility [1]. Among the most popular methods used to generate a dynamical computation are mean field descriptions (such as Landau-Vlasov, Boltzman-Uehling-Uhlenbeck, etc.), in which a generated phase-space density is followed in time, and molecular dynamics approaches [such as quantum molecular dynamics (QMD) or fermion molecular dynamics (FMD)], in which all the individual nucleons are followed as independent systems.

A nuclear collision at intermediate energies may be pictured as a series of different physical scenarios. Before the collision the projectile and target are in their ground states. After the contact they interpenetrate and a highly excited and compressed zone is created. Subsequently expansion and cooling occur, leading to the formation of exited fragments that further evolve and deexcite while departing from the collision zone. To develop a dynamical theory that includes these scenarios is a difficult task and so far no single model has been able to adequately describe all three stages. For example, statistical models for nuclear deexcitation do not address how the equilibrated source was formed, and microscopic dynamical simulations, good for the description of the early stages of the reaction, fail to reproduce the formation of complex fragments and their characteristics. This is either because of intrinsic limitations (as in mean field descriptions) or because of a lack of identification efficiency (as for molecular dynamics). A first approximation to solve this problem is to link the dynamical description of the system to a deexcitation procedure by some intermediate stage [2–5] which treats the formation of clusters of nucleons. This paper is focused towards developing a method for accomplishing this intermediate step. Although the dynamical model used in this work is a mean field type, this clusterization method can also be applied to a molecular dynamics computation.

A standard nuclear Boltzman-Uehling-Uhlenbeck (BUU) simulation is based on the solution of the modified Vlaslov transport equation for the phase-space distribution of nucleons [6]. A common method to solve the BUU equation is by the generation of an ensemble of $\mathcal{N}$ sets of dynamically independent parallel systems of $\mathcal{M}$ pseudonucleons or test particles. There are two main questions concerning the clusterization of the nucleon distributions coming from this type of calculation. One is when to stop the dynamical calculation; the other is how to proceed with actual clusterization given the output variables of the model. To deal with these questions the variables relevant to the computation must be addressed at two different levels.

At one level are the variables that describe the motion of the pseudonucleons, or test particles, in a set of parallel systems. Provided that the pseudonucleons obey the Newtonian equations of motion

$$\frac{d\mathbf{p}_i^{(n)}}{dt} = -\nabla_r U(\mathbf{r}_i^{(n)};t) \quad \text{and} \quad \frac{d\mathbf{r}_i^{(n)}}{dt} = \frac{\mathbf{p}_i^{(n)}}{m_i}, \tag{1}$$

where $\mathbf{p}_i$ is the particle momentum, $\mathbf{r}_i$ is the position, and m_i is the particle mass, the test particles will define a total phase-space distribution. This distribution is in turn a function of the second level variables that govern the evolution of the system as a collective ensemble via the BUU transport equation [6,7]

$$\left\{ \frac{\partial}{\partial t} + \frac{\mathbf{p}}{m}\cdot\nabla_r - \nabla_r U(\mathbf{r};t)\cdot\nabla_p \right\} f(\mathbf{r},\mathbf{p};t) = \overline{I[f]}, \tag{2}$$

where $\overline{I[f]}$ represents the average rate of change of the particle distribution due to two-particle collisions, $U(\mathbf{r};t)$ is the density-dependent mean field potential, and $f(\mathbf{r},\mathbf{p};t)$ is the phase-space distribution.

The collective ensemble described by Eq. (2) will follow a mean field trajectory, from which the average properties of the heavy-ion collision are calculated, and the parallel systems provide the fluctuations about these averages. Recently a consent is emerging that these fluctuations should play an essential role in the fragmentation of the system [7–9]. Thus

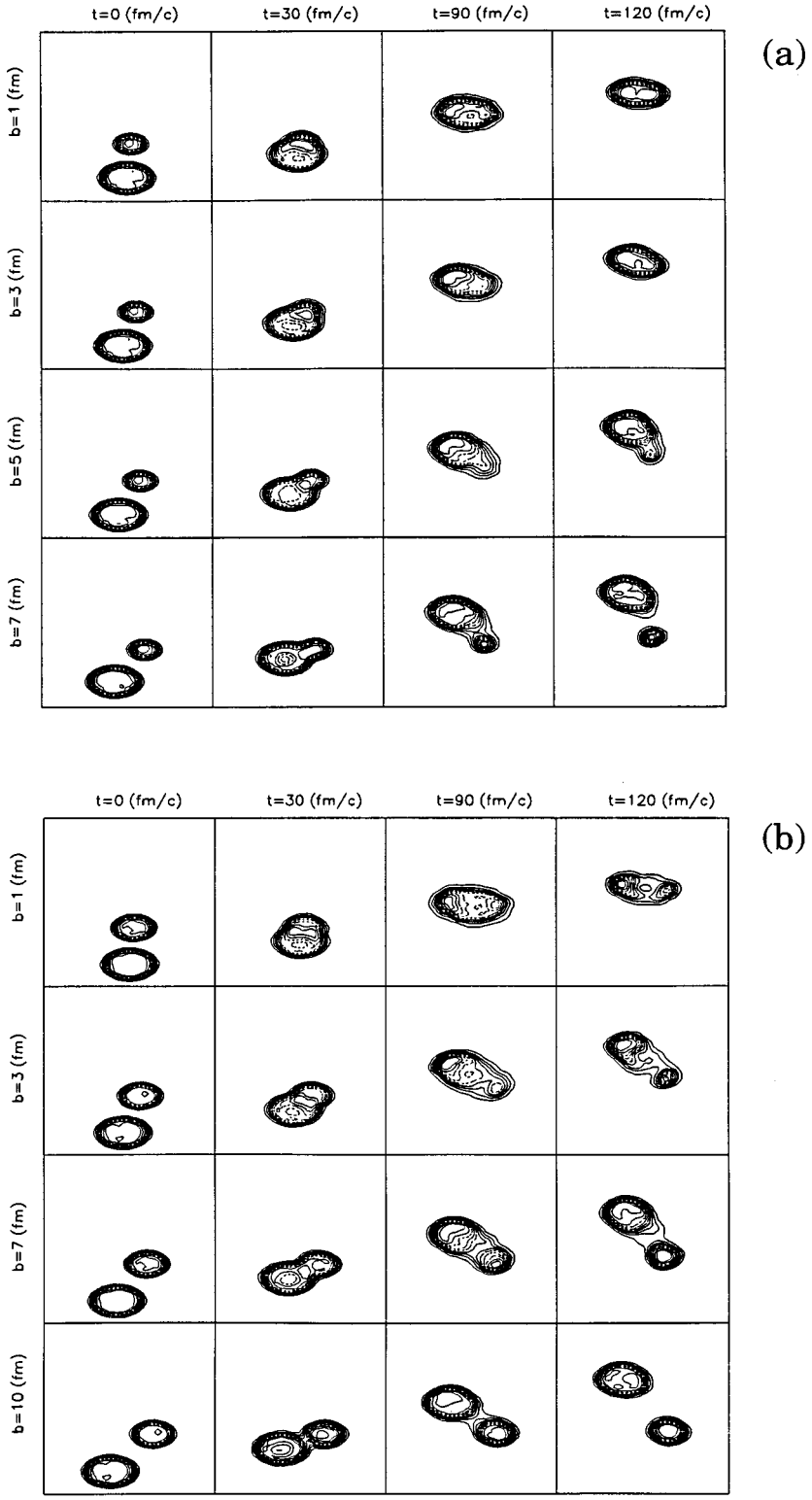

FIG. 1. Evolution predicted by the BUU simulation of the density in the reaction plane, as a function of the time and impact parameter, for the systems ^{139}La on ^{27}Al (a) and ^{nat}Cu (b) at $E/A=45$ MeV.

at some point of the dynamical calculation (freeze-out time), when these fluctuations are expected to be more prominent, the calculation is stopped, and the clusterization is applied to each of the parallel systems. From this point each member of the ensemble is treated independently [10]. It has been shown that, even though the freeze-out time depends on the system, it occurs approximately when the hot source expands to below normal nuclear density [11].

II. CLUSTERING MODEL

In order to find the freeze-out or stopping time of the calculation, it is necessary to establish the point when the fluctuations around the mean field trajectory are more pronounced. Figure 1 shows the evolution of the density function, in the plane of the reaction, as a function of time, for the systems ^{139}La on ^{27}Al and ^{nat}Cu at $E/A=45$ MeV, as

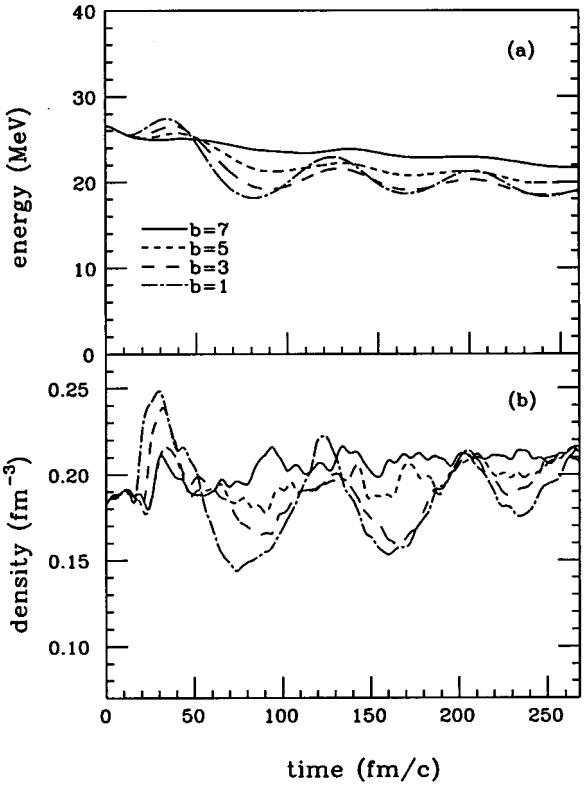

FIG. 2. Predicted average total kinetic energy (a) and maximum value of the density function (b), as a function of time, for the system ^{139}La on ^{27}Al at $E/A=45$ MeV. Each line represents the computation for different impact parameters, as defined.

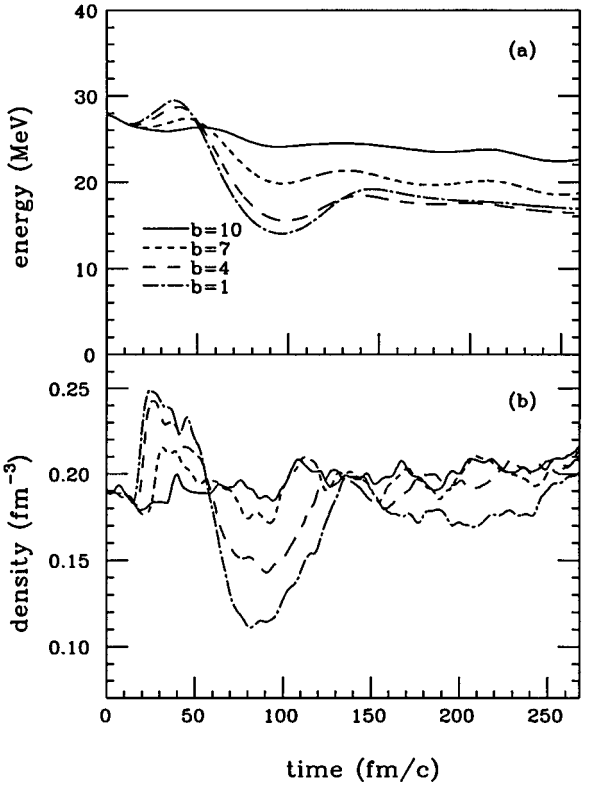

FIG. 3. Predicted average total kinetic energy (a) and maximum value of the density function (b), as a function of time, for the system ^{139}La on ^{nat}Cu at $E/A=45$ MeV. Each line represents the computation for different impact parameter ranges.

calculated from the BUU equation using $\mathcal{M}=300$ pseudoparticles. Distributions are shown for a range of input parameters and calculation times. For the smaller values of the impact parameter, where the projectile and target overlap substantially, a highly compressed system is formed. Then the system will start expanding up to a point where the compression-expansion cycle is repeated again. This is accompanied by emission of individual pseudoparticles in every cycle. At the end of the first compression-expansion cycle, when the mean field applies an inward force toward the source that cancels the outward motion, the system will spend considerable time at a relatively low density and temperature, corresponding to an unstable region in the nuclear phase diagram. Under these conditions it is expected that large first field fluctuations in the density will emerge [12], giving rise to the condensation of the system into a number of clusters. The description of this process resides outside the extent of the BUU equation, which deals only with the mean trajectory of the system, and is inadequate for descriptions of unstable evolution. Therefore, the end of the first expansion indicates an approximate time to stop the dynamical calculation and proceed with the clusterization routine.

Natural variables which can be used to estimate the freeze-out time are the density and the averaged total kinetic energy of the system. The time at which to stop the BUU calculation, $t_{\rm st}$, is therefore chosen as the time when these variables exhibit their absolute minima. The evolution as a function of time of the averaged total kinetic energy and the highest value of the density distribution computed at each time step for different impact parameters are displayed in Figs. 2 and 3 for the La on Al and Cu systems, respectively. At around 30 fm/c a highly compress system is formed, which subsequently expands, reaching a minimum in density and averaged kinetic energy at around 100 fm/c; therefore, $t_{\rm st}$ is set at 100 fm/c for both systems. It should be noted that various tests were performed changing the $t_{\rm st}$ time. It was found, in accordance with Gross *et al.* [11], that the cluster configurations remained constant within an interval of $t_{\rm st}\pm 10$ fm/c.

The common method to recognize cluster structures is to separate fragments according to the relative position in phase space of the particles in a system [10,13,14]. Using this approach, a nucleon belongs to the same cluster if it is sufficiently connected, that is

$$|\mathbf{r}_i-\mathbf{r}_j|<D_r\,, \tag{3}$$

and/or

$$|\mathbf{p}_i-\mathbf{p}_j|<D_p\,, \tag{4}$$

where $D_{r,p}$ is a parameter which is a function of the local density. Although this method is relatively simple and fast, it is not realistic if the clusters are not sufficiently well separated [3]. For example, this method is not able to separate two structures that share one surface nucleon. Strict application of Eqs. (3) and (4) will also lead to the exclusion of energetic nucleons in the clusters, therefore miscalculating

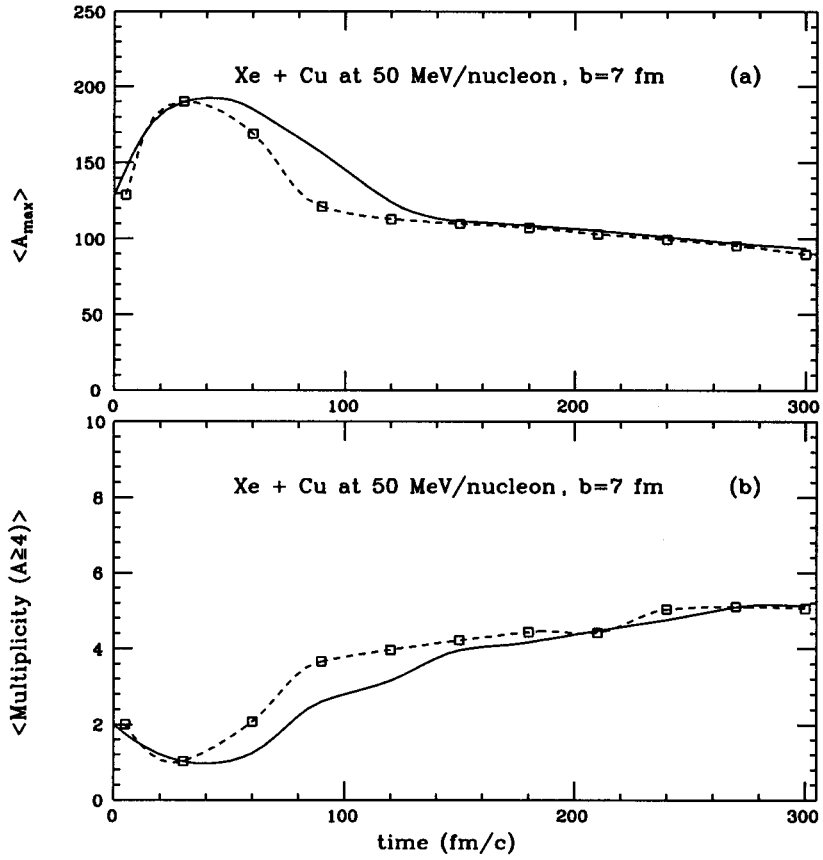

FIG. 4. Nucleon number of the largest fragment, $A_{\max}$ (a), and the multiplicity ($A \geqslant$) (b) of the clusters identified by the standard (dotted lines) and the proposed cluster method (solid line) as a function of the freeze-out time, for the system ^{129}Xe + ^{63}Cu at 50 MeV.

the amount of internal kinetic energy contained in the cluster. This latter point will be addressed again in the next section.

An alternative approach to finding the clusters without these ambiguities is to first label the interior particles in the parallel systems and then cluster them into fragment ''seeds'' using Eq. (3). To do this suppose that at $t_{\rm st}$ there is a global particle distribution $\rho(\mathbf{r})$ for the ensemble. If the coordinate space is divided into cubic cells of side $2r_b$, every cell in the space can be defined as interior or exterior to a cluster by the following condition.

Condition 1. *The cell i defined by its center at* $\mathbf{r}_i$ *will be interior if* $\rho(\mathbf{r}_i + r_b \mathbf{x}_\mu) > \rho_0$ for ever $\mathbf{x}_\mu$, $\mu = 1, \ldots, 6$ where $\mathbf{x}_\mu$ are six unitary vectors in the direction of the positive and negative axes of a coordinate space, with the positive **Z** axis directed in parallel to the beam velocity, and ρ_0 is a parameter approximately equal to 75% of the average nuclear density at the freeze-out time. Taking the position of every nucleon in each parallel system of the ensemble and applying condition 1, it is possible to determine which nucleons are, on the average, *entirely* surrounded by nuclear matter, tagging them as interior. Then, using the interior nucleons, it is possible to form the cluster ''kernel'' using a standard diagrammatic approach [14]. That is, assuming that the interior nucleons are ''slightly virtual'' and can fuse without further interaction, it is possible to apply Eqs. (3) and (4), with $D_r = r_b = 1.42$ fm, the average nuclear radius [15], to bind the initial cluster configuration.

Note that a nucleon is defined as interior by the surrounding density of its cell, not by the density within the cell. To see how this affects the clustering procedure take, for example, the system at the beginning of the dynamical calculation (second square of Fig. 1). By applying a common cluster algorithm using Eq. (3) both nuclei touching each other would be considered a single fragment. On the other hand, if the interior nucleons are separated first, then clustering would give two separated fragments, plus a number of exterior nucleons that can be treated differently.

Once the configuration of the cluster seeds for every parallel system is established, the corresponding surrounding nucleons tagged as exterior are tested by the following condition.

Condition 2. *The exterior nucleon i belongs to the cluster j if*

$$s_i \leqslant R^j_{\rm cl} + r_b$$

and

$$|\mathbf{P}^j_{\rm c.m.} - \mathbf{p}_i|, \leqslant \sqrt{p(s_i)^2_{\rm Fermi} + 2m_i[BE + E^i_{\rm Co}]},$$

where $R^j_{\rm cl}$ and $P^j_{\rm c.m.}$ are the radius and the center-of-mass momentum for the j cluster, respectively, $p(s_i)_{\rm Fermi}$, $p(s_i)_{\rm Fermi}$, m_i, $\mathbf{p}_i$, and s_i are the Fermi momenta, mass, and relative distance to the cluster center of the nucleon i, respectively. The nucleon binding energy is given by an average value of $BE = -8.0$ MeV and the Coulomb energy is $E^i_{\rm Co} = 5$ MeV for i protons and 0 MeV for neutrons. For nucleons that, by condition 2, belong to two clusters, a random assignment is made. After the first pass using condition 2, the procedure is repeated for the remaining exterior nucleons, computing the new values of the center-of-mass position

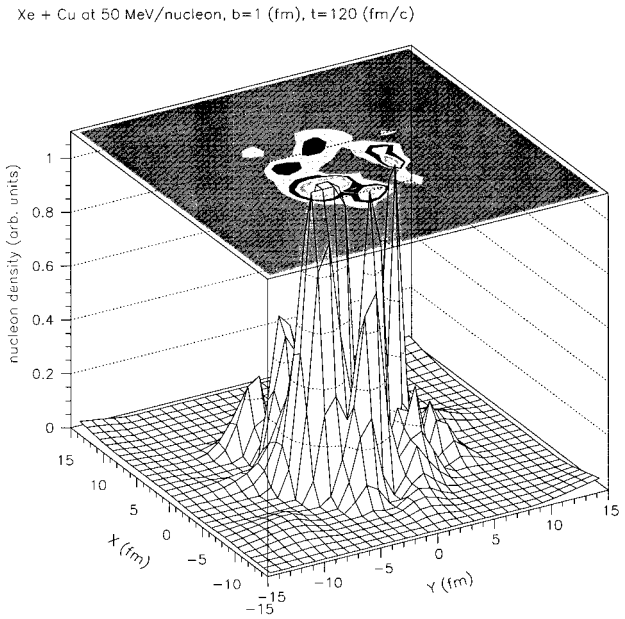

FIG. 5. Example of the cluster distribution found for one event in the reaction ^{129}Xe + ^{63}Cu at 50 MeV, at $t=120$, and impact parameter of $b=1$ fm. The X-Y axes represent the spatial location of the event, and the Z axis is the nucleon density projected in the horizontal plane. Using the standard separation method one cluster is identified.

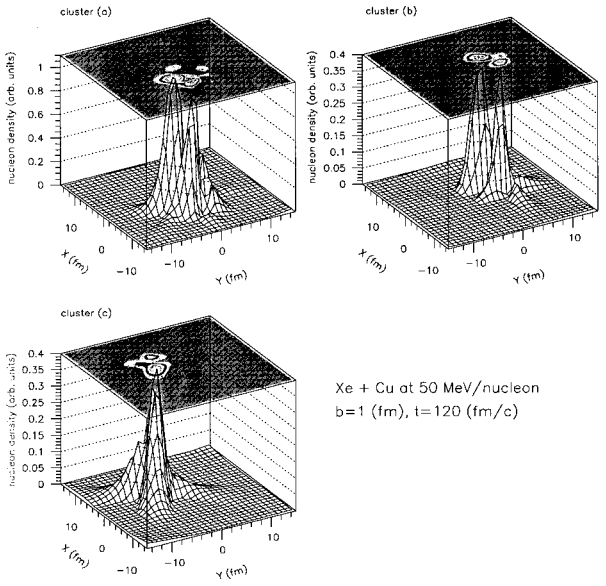

FIG. 6. Example of the cluster distribution found for one event in the reaction ^{129}Xe + ^{63}Cu at 50 MeV, at $t=120$, and impact parameter of $b=1$ fm. The X-Y axes represent the spatial location of the event, and the Z axes is the nucleon density projected in the horizontal plane. Using the proposed method the three clusters (a), (b), and (c) are identified.

and momentum at every iteration, until convergence to a constant mass of the clusters is achieved. The nucleons that, at this point, do not belong to any cluster are tagged as free. Finally, for those remaining free nucleons a coalescence check is done by using Eqs. (2) and (3).

When the configuration of the cluster is established, the collective properties for every cluster, such as translational kinetic energy, angular momentum, excitation energy, etc., are computed by using standard semiclassical formulas. Because of the instability of the cluster formed, it is not possible to know the exact zero point of the potential energy [12]. Thus, a parameter χ had to be introduced to calculate the excitation energy

$$E^*=E^*_{\rm kin}-\chi E^*_{\rm Fermi}, \tag{5}$$

where $E^*_{\rm kin}$ is the excitation energy due to the internal kinetic energy of the test particles and $E^*_{\rm Fermi}$ is the average Fermi energy of the nuclei. The parameter χ is chosen in such way that the ground state $E^*=0$ for the nuclei before the interaction. A typical value of $\chi=0.40$ was found.

III. ILLUSTRATIVE RESULTS AND COMPARISON TO STANDARD CLUSTER ANALYSIS

In order to illustrate the cluster recognition model, it is applied to the BUU simulation of the system ^{129}Xe + ^{63}Cu at 50 MeV. Figure 4 shows the nucleon number of the largest cluster, $A_{\rm max}$ (a), and the multiplicity of the clusters containing four or more nucleons (b) as a function of time. These results are the average over 300 simulations of peripheral collisions (impact parameter $b=7$ fm). For reference, in Fig. 4 the results of the cluster distribution obtained from standard spatial cluster analysis [using Eqs. (3) and (4)] are also represented (dotted lines). As expected, both methods converge on the same cluster configuration. This because the large impact parameter allows the clusters to be well separated in phase space after sufficiently large time intervals. This does not happen for earlier times; the standard cluster analysis is not able to separate clusters that are overlapped in phase space. By contrast, the method proposed is able to recognize the cluster structure much earlier. This considerably reduces the computation time, and also confirms that a cluster distribution is established relatively early in the dynamical simulations [3,16].

It must be pointed out that the contrast exhibited by the two methods of cluster recognition is exacerbated for simulations of nuclei collisions at lower impact parameters (central collisions). Figures 5 and 6 show examples of the cluster distributions found for one event in the reaction ^{129}Xe + ^{63}Cu at $E/A=50$ MeV, at $t=120$, and impact parameter of $b=1$ fm. The X-Y axes represent the spatial location of the event, and the Z axis the nucleon density projected in the horizontal plane. As can be seen in Fig. 5, it is not possible to separate the clusters formed in the toroidlike structure delivered by the BUU calculation using a standard recognition model. This method is not able to discriminate between clusters that are overlapped in phase space, and its use would lead to a single product fragment. On the other hand, Fig. 6 represents the spatial location and projected nucleon density of the three clusters ($A\geq 4$) identified by the routine proposed in this paper [(a), (b), and (c)]. This method is able to reproduce a fragment distribution that is closer to what has been observed experimentally [17].

IV. APPLICATIONS

In this section, the results of the simulation of the reactions ^{139}La on ^{27}Al and $^{\rm nat}$Cu at $E/A=45$ MeV are com-

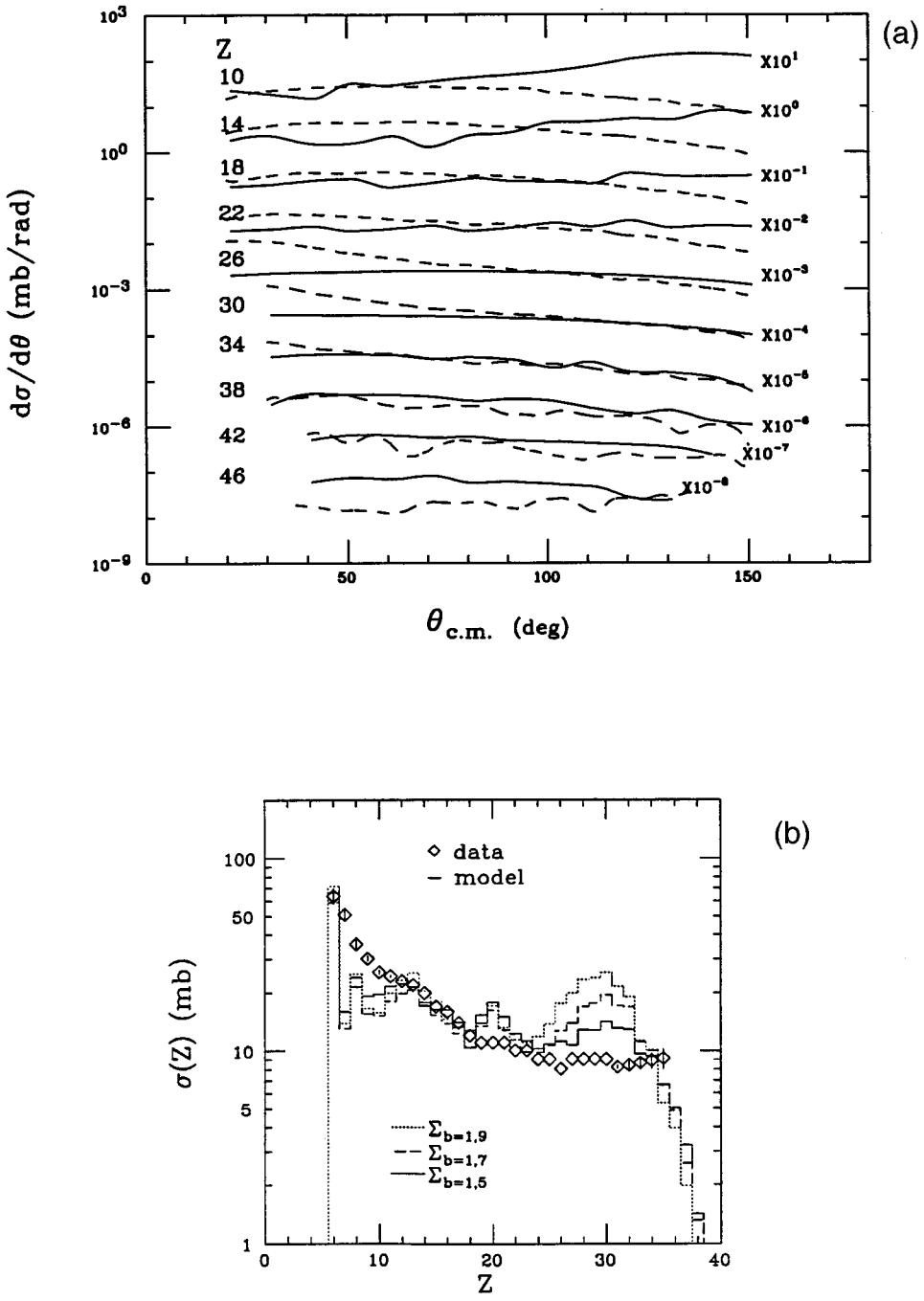

FIG. 7. Angular distributions for selected Z values (a) and integrated charge distributions (b) for the reaction La + Al at $E/A = 45$ MeV/nucleon. For the angular distributions, the experimental (solid lines) and calculated (dashed lines) values are defined in the center of mass. For the total cross section, the experimental data are represented by diamonds and the calculated distributions are represented by solid, dashed, and dotted lines, for integration over different impact parameter ranges.

pared to experimental data [17] after running through the evaporation code GEMINI [18]. The model cross sections and angular distribution as a function of the detected charge were calculated directly from the output of the evaporation code. On the other hand, the velocity distributions and sum charge yields for different multiplicity gates were filtered according to the corresponding experimental setup.

The results of the model calculation, together with the experimental data, are shown in Figs. 7 to 10. Figures 7 and 8 show the angular distributions and integrated charge distributions for the Al and Cu targets, respectively. For each system an overall normalization was used for the calculated angular distributions, and the integrated charge distributions were normalized individually for the different impact parameter ranges.

For the Al target, the angular distributions [Fig. 7(a)] for the heavier fragments $Z = 42$ down to $Z = 34$ are fairly reproduced by the calculations. On the other hand, for the range $Z = 34-22$, the model overpredicts the yield at forward angles. After $\theta_{\text{c.m.}} = 50°$ the calculations again correspond to the experimental data. For Z values smaller than 20, the contrary trend is found; the model replicates well the data up to $\theta_{\text{c.m.}} = 50°$ and after this it underpredicts the yield.

In Fig. 7(b) the experimental Z distribution in cross section is compared to the model predictions. The solid and dashed lines represent the cross sections integrated over different intervals of impact parameter, each one normalized separately. In general, the cross sections agree reasonably well with the experimental data. However, for $Z = 7-10$ the model underpredicts the yield, and a bump is observed

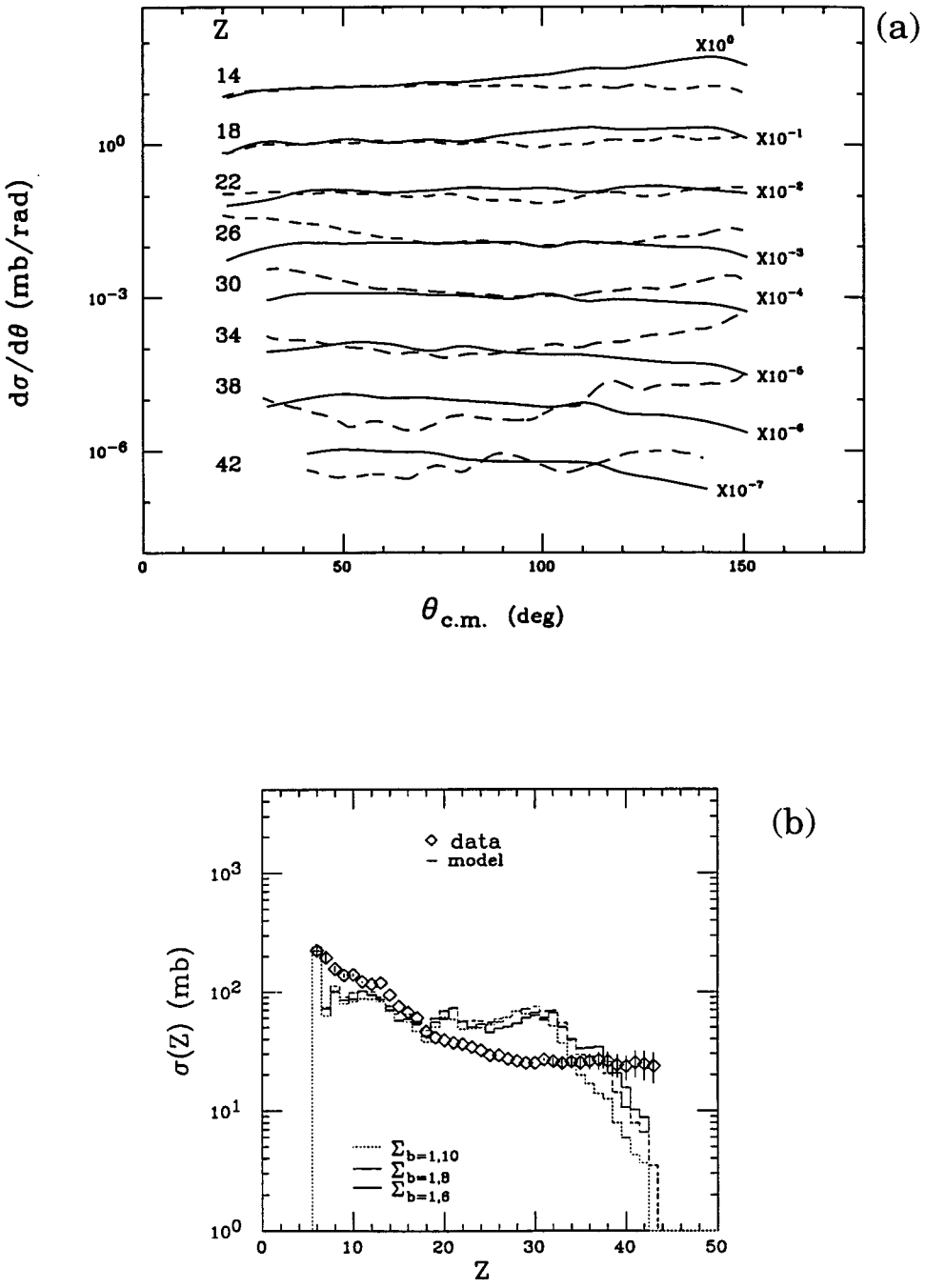

FIG. 8. Angular distributions for selected Z values (a) and integrated charge distributions (b) for the reaction La + Cu at $E/A = 45$ MeV. For the angular distributions, the experimental (solid line) and calculated (dashed lines) values are defined in the center of mass. For the total cross section, the experimental data are represented by diamonds and the calculated distributions are represented by solid, dashed, and dotted lines, for integration over different impact parameters.

around $Z = 30$. This bump grows proportionally to the interval of integration and may indicate that the fitting of the experimental angular distribution used to calculate the cross section was biased to exclude the fragments from more peripheral reactions, which are very forward peaked.

The angular distributions for the Cu [Fig. 8(a)] target show the same general behavior as for the Al target, except for the overprediction of the calculation for fragments with $Z \geqslant 32$ at the backward angles. For the smaller fragments, the calculation better fits the data for $\theta_{\text{c.m.}} \geqslant 100°$. The bump in the integrated cross sections around $Z = 32$ remains almost constant with increasing integration interval, and the cross section increases for larger integration intervals for fragments with $Z \geqslant 36$. This component may again be interpreted as a residue of the projectile from peripheral reactions.

The sums of the detected charge and the source velocity distributions, for all coincidence events with multiplicity $n = 2$ and $n = 3$, are shown in Figs. 9 and 10. The dashed lines represent the calculated distributions and the solid lines the data. In general, for the $n = 2$ events, the peak in the Z_{tot} distribution is fairly reproduced by the calculation. The tail of the distribution is overpredicted for the Al target, and the central part of the distribution is underpredicted for the Cu target. For $n = 3$ events, the model is able to predict the position of peak of the Cu distribution; however, it underestimates the width and the tale of the distribution. On the other hand, the model is able to reproduce the peaks of the V_S distributions to within a few percent, also reproducing the width and the tail for $n = 2$ events for the Cu target. However, the width is overpredicted for the Al target. For $n = 3$

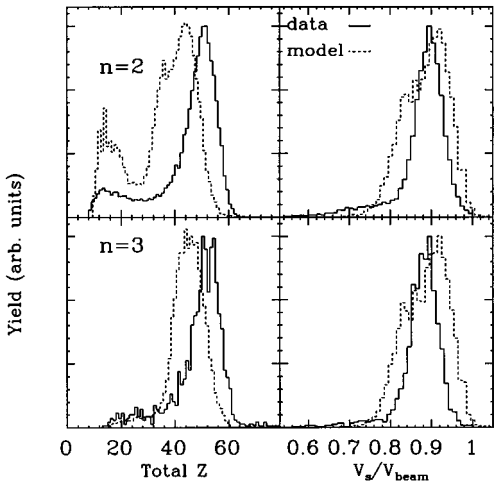

FIG. 9. Experimental (solid lines) and calculated (dashed lines) sums of the detected charge and source velocity distributions, expressed in velocity relative to the beam velocity V_s, for $n=2$ and 3 events for the reaction La + Al at $E/A=45$ MeV.

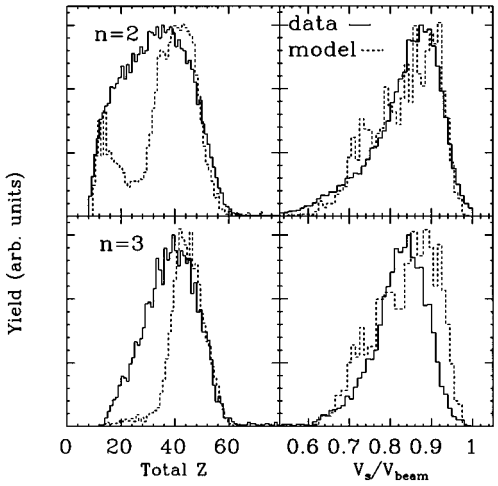

FIG. 10. Experimental (solid line) and calculated (dashed line) sums of the detected charge and source velocity distributions, expressed in velocity relative to the beam velocity V_s, for $n=2$ and 3 events for the reaction La + Cu at $E/A=45$ MeV.

events, the widths are also overpredicted, and the peak is shifted to higher velocities for both targets.

V. CONCLUSION

In this work, a dynamical description of nucleus-nucleus collisions was coupled with a subsequent statistical decay of the primary source through a clustering subroutine. The specific clustering criteria provide a reasonable approach, not only for dealing with dynamically separated clusters, but also for generally dense stages of the reaction. A significant improvement in the cluster separation is obtained as compared to results from the standard phase-space cluster analysis. Even though that the predictions provide only a qualitative description of the data, they represent an improvement when compared to the simulations performed for other studies [2,8,10]. The results obtained show that it is possible to describe the fragment distributions produced in intermediate energy heavy-ion reactions considering both statistical and dynamical features.

It should be pointed out that the approximation used to estimate the excitation energy of the clusters is far from optimal. Work in progress shows that using a radially dependent mean field potential to calculate the internal energy of the clusters [10] results in a reasonable temperature [19] ($E_{\rm tot}\simeq -12$ MeV/nucleon) for a nucleus in its ground state (that is BUU-generated $A+B$ nuclei at zero incident energy). This is particularly important when treating peripheral reactions. Further applications of the clusterization model described in this paper using this estimation of the excitation energy should result in more realistic predictions for these low excitation energy reactions.

Finally, it also should be mentioned that, in spite of the reasonable predictions that are obtained, this clustering routine is far from optimal because it sharply stops the dynamical calculation. Further work in this area should focus on obtaining the clusterization directly from the dynamical evolution of the density distribution of the system.

ACKNOWLEDGMENTS

The authors wish to thank W. Bauer and R. J. Charity for providing the core of the codes used in this work, and to S. Egido Arteaga for his advice. This research was supported by the U.S. Department of Energy under Grants No. DEFG05-87ER40321 and No. DEFG02-93ER40802.

[1] G.F. Bertsch and S. Das Gupta, Phys. Rep. **160**, 190 (1988).
[2] M. Colonna, M. DiToro, V. Latora, and A. Smerzi, Prog. Part. Phys. **30**, 17 (1993).
[3] C. Dorso and J. Randrup, Phys. Lett. B **301**, 328 (1993).
[4] M. Colonna, P. Roussel-Chomaz, N. Colona, M. DiToro, L.G. Moretto, and G.J. Wozniak, Phys. Lett. B **283**, 180 (1992).
[5] A. Ono, H. Horiuchi, T. Maruyama, and A. Ohnishi, Prog. Theor. Phys. **87**, 1185 (1992).
[6] Bao-An Li, W. Bauer, and George F. Beretsch, Phys. Rev. C **44**, 2095 (1991).
[7] G. Batko and J. Randrup, Nucl. Phys. **A563**, 97 (1993).
[8] D.R. Bowman, C.M. Mader, G.F. Peaslee, W. Bauer, N. Carlin, R.T. de Souza, C.K. Gelbke, W.G. Gong, Y.D. Kim, M.A. Lisa, W.G. Lynch, L. Phair, M.B. Tsang, C. Williams, N. Colonna, K. Hanold, M.A. McMahan, G.J. Wozniak, L.G. Moretto, and W.A. Friedman, Phys. Rev. C **46**, 8834 (1992).
[9] L. Phair, W. Bauer, and C.K. Gelbke, Phys. Lett. B **314**, 271 (1993).
[10] J.P. Whitfield and N.T. Porile, Phys. Rev. C **49**, 304 (1994).
[11] D.H.E. Gross, Bao-An Li, and A.R. DeAngelis, Ann. Phys. (N.Y.) **1**, 467 (1992).
[12] J. Randrup and G. Batko, Prog. Part. Nucl. Phys. **30**, 117 (1993).
[13] M. Colonna, N. Colonna, A. Bonasera, and M. DiToro, Nucl. Phys. **A541**, 295 (1992).

[14] V.M. Kolybasov and Yu.N. Solokol'skikh, Sov. J. Nucl. Phys. **55**, 1148 (1992).
[15] H. Hauser and H. Feshbach, Phys. Rev. **87**, 366 (1952).
[16] A. Aranda, C.O. Dorso, V. Furci, and J.A. Lopez, Phys. Rev. C **52**, 3217 (1995).
[17] P. Roussel-Chomaz, N. Colonna, Y. Blumenfeld, B. Libby, G.F. Peaslee, D.N. Delis, K. Hanold, M.A. McMahan, J.C. Meng, Q.C. Sui, G.J. Wozniak, L.G. Moretto, H. Madani, A.A. Marchetti, A.C. Mignerey, G. Guarino, N. Santoruvo, I. Iori, and S. Bradley, Nucl. Phys. **A551**, 508 (1993).
[18] R.J. Charity, Nucl. Phys. **A483**, 371 (1988); **A511** 59 (1990).
[19] C. Dorso and J. Randrup, Phys. Lett. B **215**, 611 (1988).